Coupling alongshore variations in wave energy to beach morphologic change using the SWAN wave model at Ocean Beach, San Francisco, CA

Jodi L. Eshleman, Patrick L. Barnard, Li H. Erikson and Daniel M. Hanes

United States Geological Survey, Coastal and Marine Geology Program
Pacific Science Center, 400 Natural Bridges Drive, Santa Cruz, CA 95060
jodieshleman@hotmail.com

1.0 INTRODUCTION

Coastal managers have faced increasing pressure to manage their resources wisely over the last century as a result of heightened development and changing environmental forcing. It is crucial to understand seasonal changes in beach volume and shape in order to identify areas vulnerable to accelerated erosion. Shepard (1950) was among the first to quantify seasonal beach cycles. Sonu and Van Beek (1971) and Wright et al. (1985) described commonly occurring beach states. Most studies utilize widely spaced 2-D cross shore profiles or shorelines extracted from aerial photographs (e.g. Winant et al., 1975; Aubrey, 1979; Aubrey and Ross, 1985; Larson and Kraus, 1994; Jimenez et al., 1997; Lacey and Peck, 1998; Guillen et al., 1999; Norcross et al., 2002) to analyze systematic changes in beach evolution. But with the exception of established field stations, such as at Duck, NC (Birkemeier and Mason, 1984), and Hazaki Oceanographical Research Station (HORS) in Japan (Katoh, 1997), there are very few beach change data sets with high temporal and spatial resolutions (e.g. Dail et al., 2000; Ruggiero et al., 2005; Yates et al., in press). Comprehensive sets of nearshore morphological data and local in situ measurements outside of these field stations are rare and virtually non-existent on high-energy coasts. Studies that have attempted to relate wave statistics to beach morphology change require some knowledge of the nearshore wave climate, and have had limited success using offshore measurements (Sonu and Van Beek, 1971; Dail et al., 2000).

The primary objective of this study is to qualitatively compare spatially variable nearshore wave predictions to beach change measurements in order to understand the processes responsible for a persistent erosion 'hotspot' at Ocean Beach, San Francisco, CA. Local wave measurements are used to calibrate and validate a wave model that provides nearshore wave predictions along the beach. The model is run for thousands of binned offshore wave conditions to help isolate the effects of offshore wave direction and period on nearshore wave predictions. Alongshore varying average beach change statistics are computed at specific profile locations from topographic beach surveys and lidar data.

The study area is located in the San Francisco Bight in central California. Ocean Beach is a seven kilometer long north-south trending sandy coastline located just south of the entrance to the San Francisco Bay Estuary (Figure 1). It contains an erosion hotspot in the southern part of the beach which has resulted in damage to local infrastructure and is the cause of continued concern. A wide range of field data collection and numerical modeling efforts have been focused here as part of the United States Geological Survey's (USGS) San Francisco Bight Coastal

Processes Study, which began in October 2003 and represents the first comprehensive study of coastal processes at the mouth of San Francisco Bay.

Ocean Beach is exposed to very strong tidal flows, with measured currents often in excess of 1 m/s at the north end of the beach. Current profiler measurements indicate that current magnitudes are greater in the northern portion of the beach, while wave energy is greater in the southern portion where erosion problems are greatest (Barnard et al., 2007). The sub-aerial beach volume fluctuates seasonally over a maximum envelope of 400,000 m^3 for the seven kilometer stretch (Barnard et al., 2007). The wave climate in the region is dominated by an abundance of low frequency energy (greater than 20 s period) and prevailing northwest incident wave angles. The application of a wave model to the region is further complicated by the presence of the Farallon Islands 40 kilometers west, and a massive ebb tidal delta at the mouth of San Francisco Bay (~ 150 km^2), which creates complicated refraction patterns as wave energy moves from offshore into Ocean Beach. In situ measurements of waves and currents have been collected at Ocean Beach; however the cost and threat of the energetic nearshore environment have limited the temporal and spatial resolution of these measurements. Applying numerical models to predict wave and current patterns along the beach can help supplement the field data that exists and provide opportunities to make predictions about the impacts of changing environmental forcing.

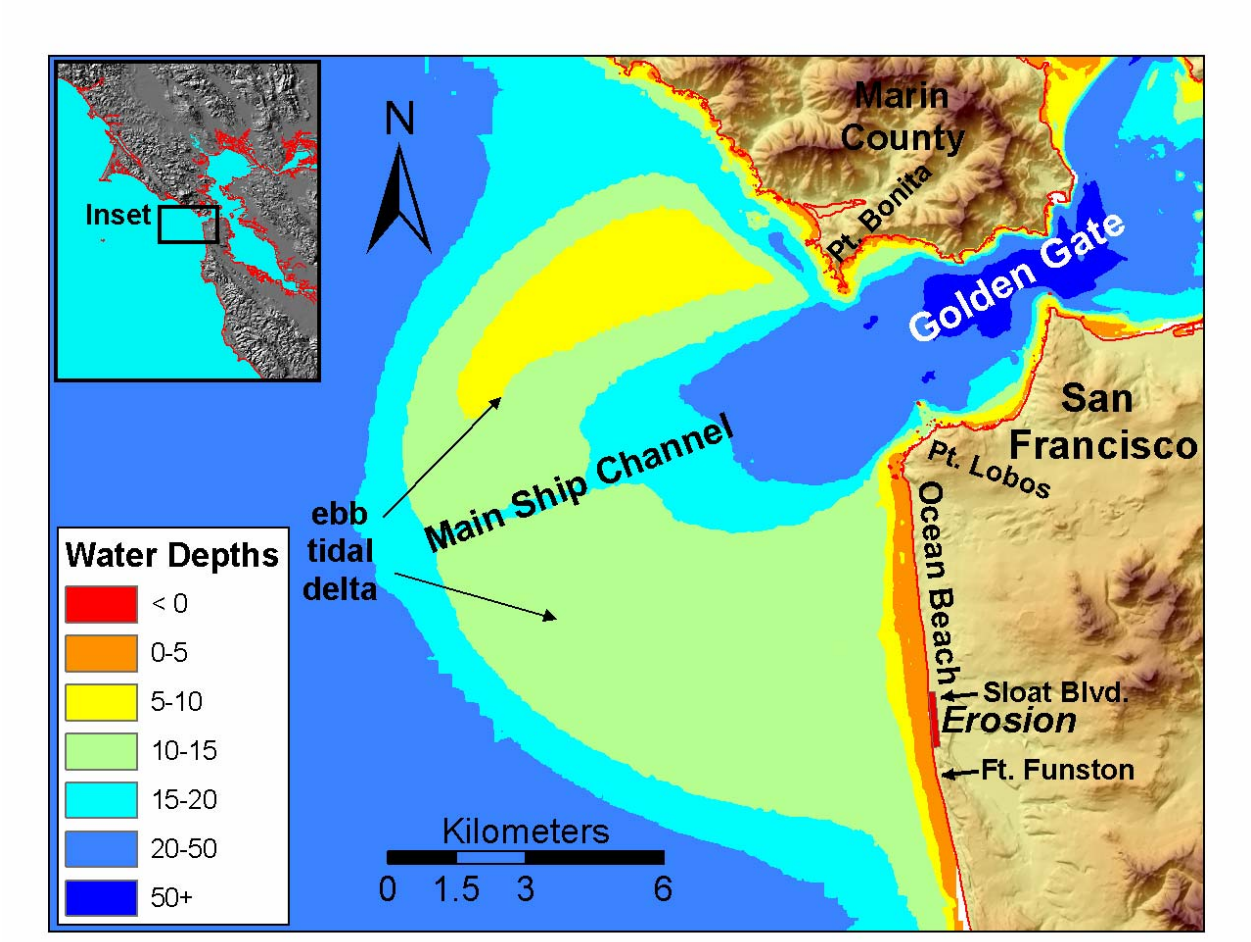

Figure 1. Map of the study area.

2.0 METHODS

The goal of this study is to compare measurements of beach change to local wave forcing in order to understand why certain sections of Ocean Beach have experienced persistent erosion. We accomplish our goal by generating spatially variable nearshore wave predictions and qualitatively comparing these to average beach statistics. Nearshore circulation patterns appear to be highly spatially variable along the beach. As a result, a numerical model is applied to give a more complete spatial description of nearshore forcing than discrete measurements can provide, since there are only a few instrument sites for the entire seven kilometer stretch at Ocean Beach.

2.1 SWAN Model Application

A SWAN wave model (Delft University, 2007) was applied with a nested grid setup (Figure 2) to model wave propagation within the San Francisco Bight. The outer grid (Grid 1) extends past the continental shelf to a depth of over 3500 meters to avoid boundary problems resulting from the combination of an angled coastline and a steep angle of wave incidence (Figure 3a). This outer grid has a 500 m resolution. Three smaller grids of consecutively finer resolution (Grids 2, 3, and 4) cover the remaining area from west of the Farallon Islands to Ocean Beach, with resolutions of 200 m, 100 m, and 25 m, respectively (Figure 2). It was necessary to have four nested grids in order to achieve the desired resolution at Ocean Beach and capture the shadowing effects caused by the Farallon Islands (Figure 3b). The Farallon Islands are very small; however, they have a very large impact on waves, and grids with coarser resolution than 200 m could not account for their influence. A curvilinear grid with increasing resolution moving shoreward would be more time efficient in this application since only one model run is required for each wave condition. However, previous research suggests that when incidence wave angles align with grid cell orientation, model convergence problems can result (Delft Hydraulics, personal communication), so rectilinear grids were used in this study. The bathymetry files originate from the following data files in order of importance; nearshore bathymetry survey data collected by the Coastal Profiling System (CPS; Ruggiero et al., 2005) from 2004 through 2006, multibeam data of the ebb tidal delta and inlet from 2004-05 collected by the USGS Coastal and Evolution Modeling Project, and multibeam and echosounder data collected by the National Marine Sanctuary Program in 2003.

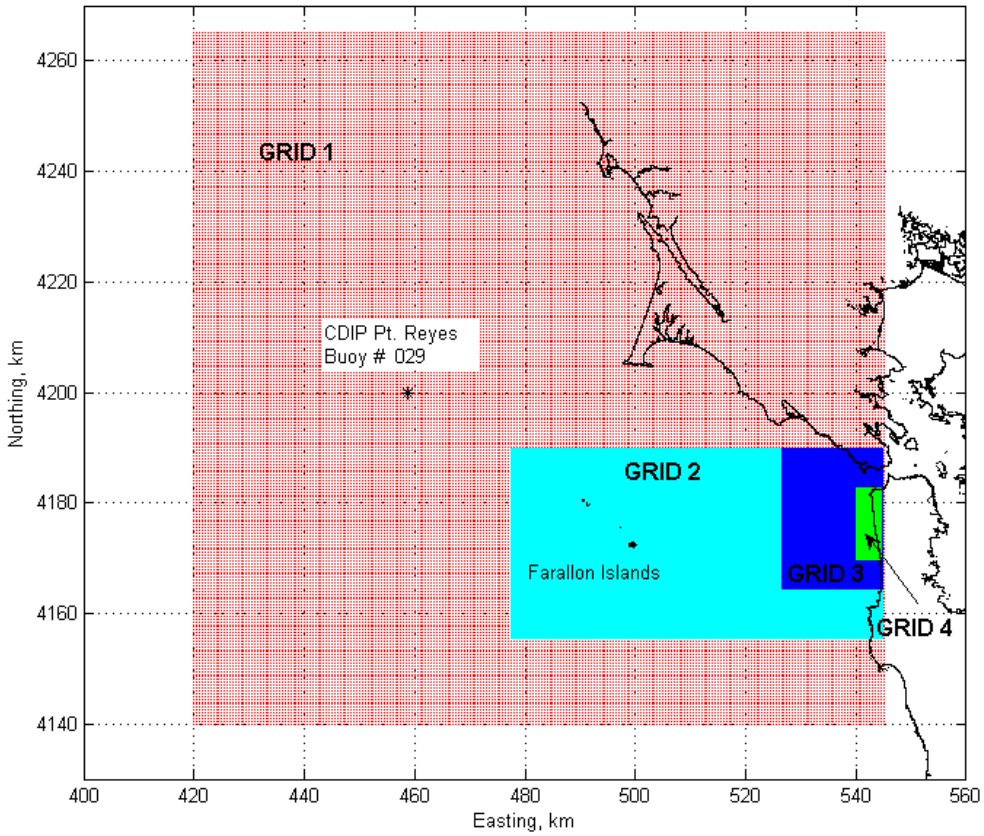

Figure 2. Nested SWAN grids along with location of CDIP Point Reyes buoy used to force the model (Scripps, 2006).

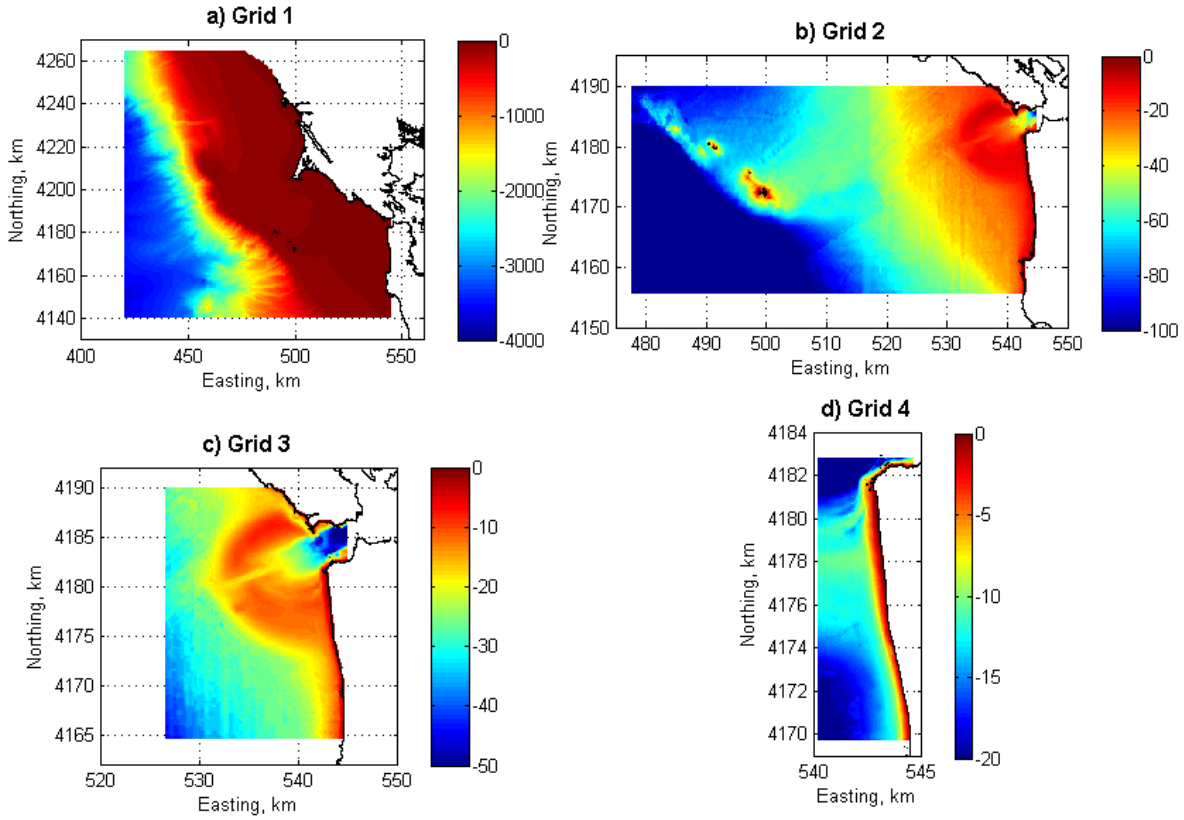

Figure 3. Depth in meters relative to NAVD88 for SWAN a) Grid 1 with 500 m resolution b) Grid 2 with 200 m resolution c) Grid 3 with 100 m resolution and d) Grid 4 with 25 m resolution.

The Coastal Data Information Program (CDIP) has a Datawell directional wave buoy (#029) located in 550 m water depth off of Point Reyes, CA that provides valuable information about the offshore wave climate (Scripps, 2006; Figure 2). Measurements from this buoy were used to force the model on all three open boundaries. There were two different data sets chosen to validate the wave output from SWAN, which include wave and current profiler measurements at five different instrument sites from summer 2005 and winter 2006. Figure 4 includes information about the location of these instruments offshore of Ocean beach and bathymetry for nearby SWAN grids 3 and 4. Six test cases were chosen for model validation and represent three times during each field deployment when measurements at the CDIP Pt. Reyes buoy represented a range of offshore wave conditions. SWAN version 40.51 was run in stationary mode for each test case, with full 2d forcing applied at each offshore boundary using the MEM directional spectra reported by CDIP (Scripps, 2006). A current grid was generated with the Delft3d Flow model for the same region and applied to account for strong tidal currents (Delft3D, 2006). A sensitivity analysis helped to determine which formulations and constant values had the greatest effect on the model output for Grid 4 at Ocean Beach, and the results were applied to calibrate the wave model for a friction coefficient using the Madsen formulation with varied values for Nikuradse roughness (Delft, 2007).

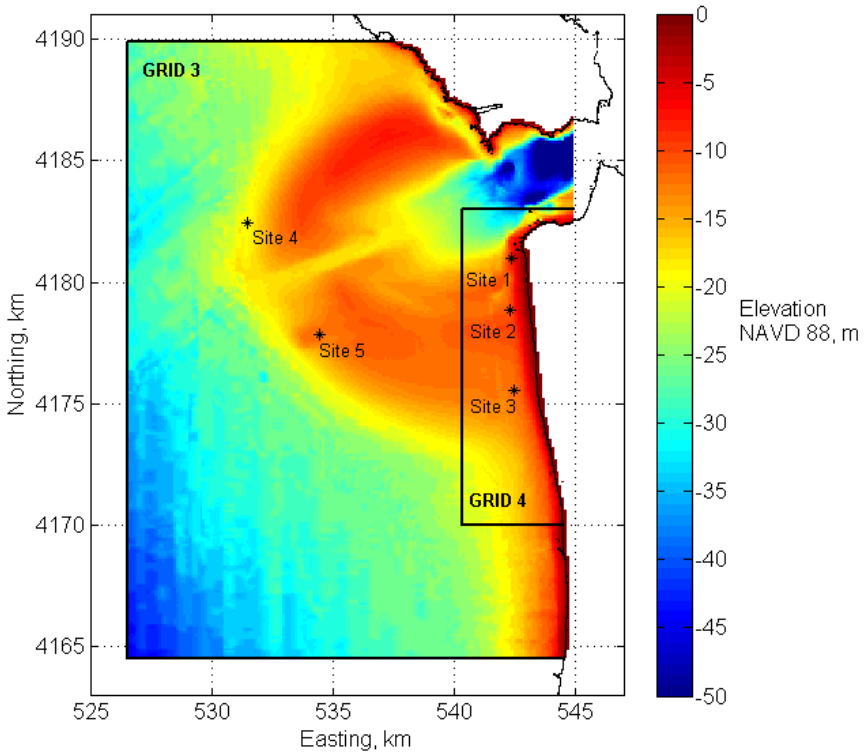

Figure 4. Locations of current profilers at Ocean Beach with local bathymetry and the outline of Grids 3 and 4 included as solid black lines.

All values that were modified from the default setup are discussed below. The inrhog command was set to 0 so that our spectral output was based on variance, which facilitated comparisons with measured spectral information. The nautical convention for wind and wave direction was chosen to be consistent with oceanographic measurements. A low frequency cutoff of 0.03 Hz was applied since waves with peak periods greater than 20 seconds are often measured in this region and we didn't want to lose low-frequency spectral information for those cases. The high frequency cutoff was set to 0.3 Hz, since wave measurements often showed energy out at that frequency. We used 48 frequency bins and 72 directional bins in the full circle, giving 5 degree directional resolution and providing similar coverage to measured values in both frequency and directional space. The model was run in generation 3 mode, with the Janssen formulation applied for linear growth and whitecapping. Wind was not included and quadruplet wave-wave interactions were not activated. The Madsen friction formulation was applied with a calibrated roughness length scale of 0.01 m. The convergence criteria were modified to require 99% of cells to meet the convergence requirement or a maximum of 50 iterations. This resulted from previous testing that showed that a 95% convergence requirement sometimes allowed cells that did not fully converge at the north end of Ocean Beach and gave unrealistic results in that region.

2.2 Quantifying Beach Morphology Change

The topographic beach survey data and current profiler measurements were collected as part of the U.S. Geological Survey San Francisco Bight Coastal Processes Study, and detailed information about data collection and processing techniques can be found in Barnard et al. (2007). To help quantify spatial changes in beach shape and storage along Ocean Beach, 138 cross-shore profiles were generated every 50 m alongshore and extracted from 34 topographic surveys collected between April 2004 and August 2006. Figure 5 shows the location of these profiles along with "reach" designations, which include sections of the beach grouped based on observed similar response to variable forcing.

The cross-shore locations of 30 cm below mean sea level and the upper swash limit were used to define the profile range for profile change statistics. Since we do not have measurements of wave runup, we assume that we can estimate this upper limit by choosing the location where less sediment is moving around on the beach. In this study, the upper swash limit is defined as a pinch point where the standard deviation of elevation of all profiles is less than 25 cm. Comparisons of this location with the standard deviation of all measured elevations throughout the beach show that in the southern portion of Ocean Beach (reaches 4-7), the swash zone is cut off by a backing sea cliff, therefore, no upper swash limit can be defined using the standard deviation cutoff approach (Figure 5b). It is difficult to survey this section since there is often very little beach exposed at low tide. Therefore, the profile range in the southern portion of the beach is bounded by the location of 30 cm below mean sea level and the upper limit where data is available. This upper limit is defined by the location of 50% onshore data coverage. Several statistics were determined for each profile and for each available survey. The total beach width is the cross-shore distance between 30 cm below mean sea level and the upper swash limit. The slope of the profile is determined by taking the slope between each set of consecutive cross-shore points and averaging these slope values over the profile range. The sediment storage is defined as the cross-sectional area bounded by the total beach width region.

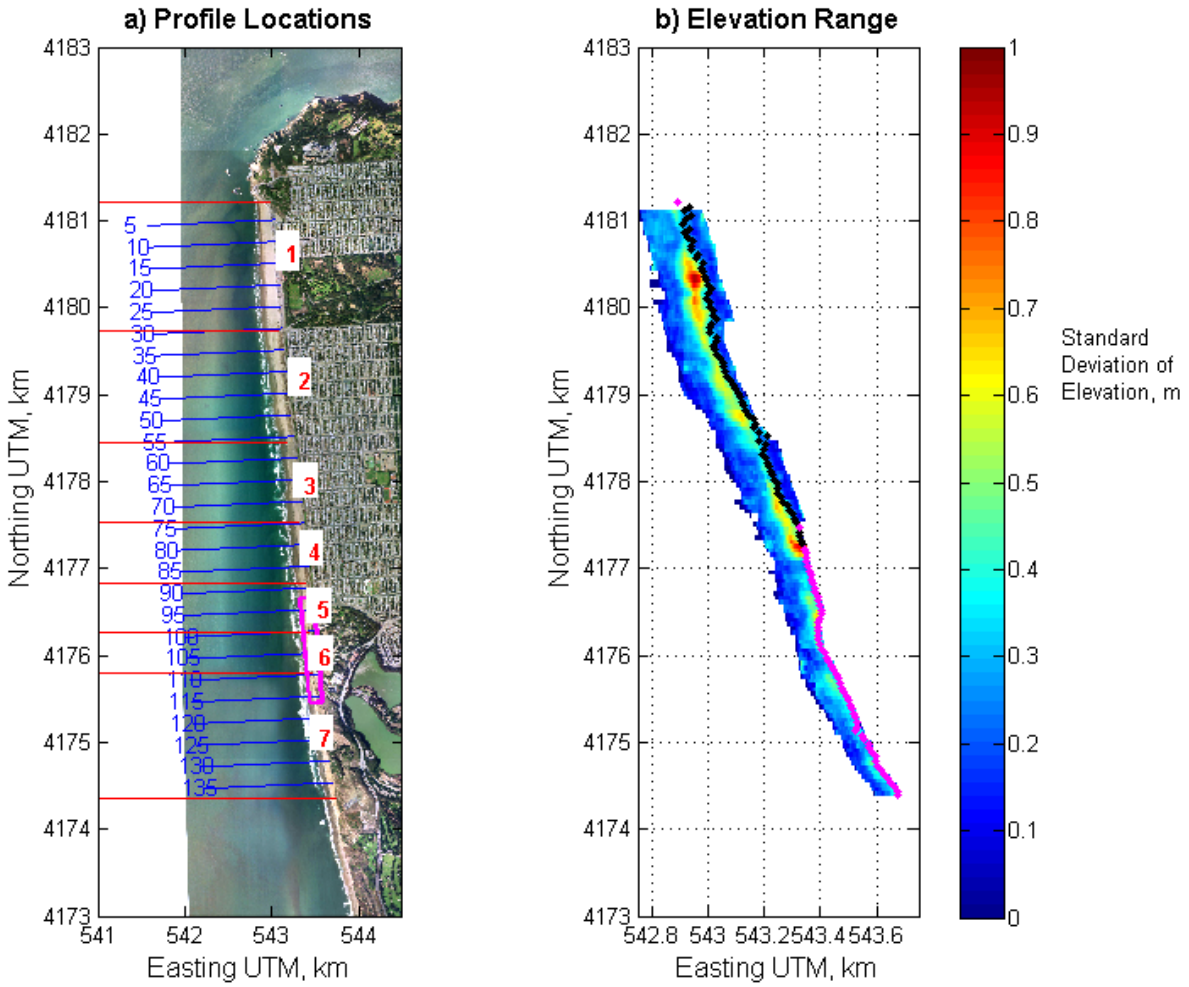

Figure 5. a) Topographic profiles used for analysis (blue lines show every fifth profile) and reach designations (red lines) for Ocean Beach. Magenta box shows location of erosion hotspot. b) Standard deviation of elevation and upper swash limit based on standard deviation (black dots) and upper data limit (magenta dots). Note that this is exaggerated in easting.

3.0 RESULTS

Current profiler measurements collected during the summer of 2005 and winter of 2006 are used to validate SWAN model output at Ocean Beach. Barnard et al., 2007 discusses the different types of instrumentation that were deployed and processing techniques applied. Comparisons focus on specific events and include spectral information to help isolate the performance of individual model processes. Average beach statistics are compared with local bathymetry and shoreline change rates. The SWAN model discussed above is run for a series of binned offshore wave conditions. Alongshore averages of wave height over different offshore wave peak direction and period bins are compared.

3.1 Model-Data Comparisons

Table 1 includes a comparison of measured and modeled bulk parameters for each of the test cases at site 3 (Figure 4). Measured and modeled times are not exactly the same as a result of varied sampling intervals for buoy forcing and current profiler measurements. Differences between measured and model output are included as a percent difference of the measured values and are shown in color. Although these parameters are useful, they do not completely describe the modeled and measured wave climate since energy at multiple frequencies and directions is often present. The corresponding 1-D spectral output for each of the six test cases is compared along with the boundary forcing in Figure 6 for site 3 at the southern end of Ocean Beach, as this is the only site where an instrument was deployed for both the summer and winter instrument campaigns. This plot shows that the model successfully captures complex refraction patterns over the ebb tidal delta and changes in energy between the offshore forcing and inshore instrument sites. However, the wave model dissipates too much of the high frequency energy when it exists (Figure 6a - c). For test case one a large portion of the energy at frequencies greater than 0.1 Hz is lost. Test case three shows this on a much smaller scale. For test case two this same thing happens at frequencies greater than 0.15 Hz. This missing high frequency energy explains the significant underestimation of the significant wave height for those cases (Table 1). The large discrepancy in wave period for test case 2 (Table 1) is a result of having a very broad spectrum with multiple peaks of similar magnitude (Figure 6b). The model jumps between peaks, but still predicts the spread of energy in frequency and direction fairly well. The largest difference in peak wave direction occurs for test case 5 (Table 1). Figure 7 includes 2-D spectral plots for this winter swell event, and this shows that the model captures the range of energy in both direction and frequency well, however maintains two peaks where the measured energy is merged into a single peak.

Table 1. Comparison of measured and modeled bulk wave parameters at site 3 for each of the six test cases used for model calibration and validation.

Test Case	Measured Time	Modeled Time	Hs, measured m	Hs, modeled m	Tp measured sec	Tp, modeled sec	Dp, measured deg	Dp, modeled deg
1	6/27/05 08:26:00	6/27/05 08:00:00	1.51	0.75	18.2	16.6	220	213
2	7/11/05 22:56:00	7/11/05 22:00:00	1.70	1.25	5.8	10.3	289	288
3	7/15/05 00:56:00	7/15/05 00:00:00	1.65	1.23	11.6	10.9	286	298
4	1/13/06 22:00:00	1/13/06 22:00:00	1.90	2.17	18.2	16.3	228	243
5	1/29/06 18:30:00	1/29/06 18:00:00	2.36	2.00	11.6	12.5	279	248
6	2/5/06 07:00:00	2/5/06 06:00:00	3.77	3.32	16.0	14.8	238	238

red = model comparison to measurement (>±20% difference)
blue = model comparison to measurement (>±10% and <±20% difference)
green = model comparison to measurement (<±10% difference)

Testing revealed that the model's tendency to dissipate too much energy at frequencies greater than 0.1 Hz is not caused by frictional dissipation, the whitecapping formulation, or stationary effects alone and the energy begins to decay immediately after the boundary forcing is applied in deep water. Since we have not isolated the cause of this high-frequency dissipation, it is important to be aware of this current limitation of model capability. The model generally underestimates the amount of wave energy at all sites; although it does a good job of representing the spectral shape and transferring energy to the nearshore in very large winter swell events (Figure 6d-e), where all bulk parameters are within 20% of measured values, and many are within 10% (Table 1).

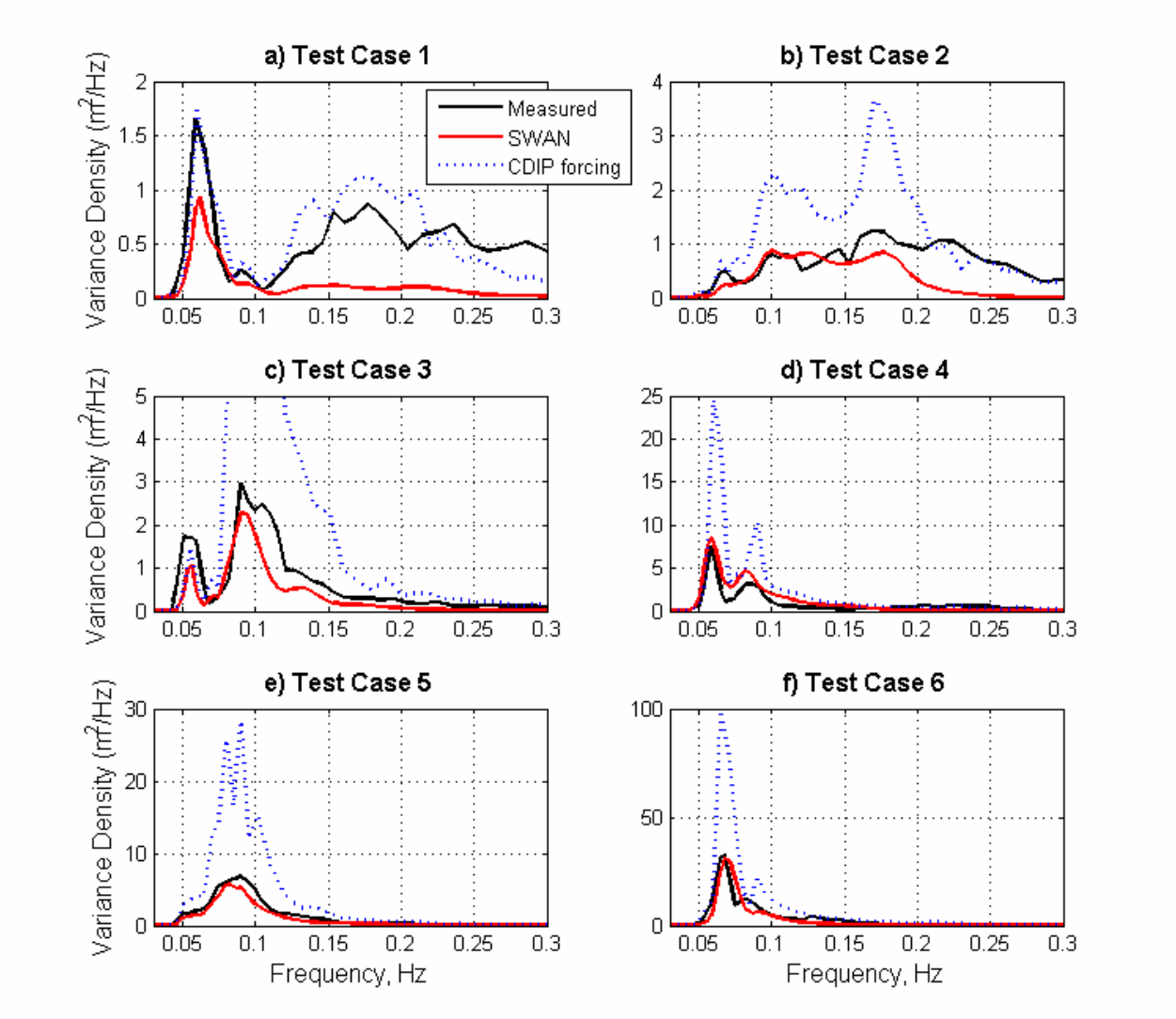

Figure 6. Comparisons of measured and modeled energy spectra at Site 3 with boundary forcing for a) test case 1, b) test case 2, c) test case 3, d) test case 4, e) test case 5, and f) test case 6 (Note the different scale; Scripps, 2006).

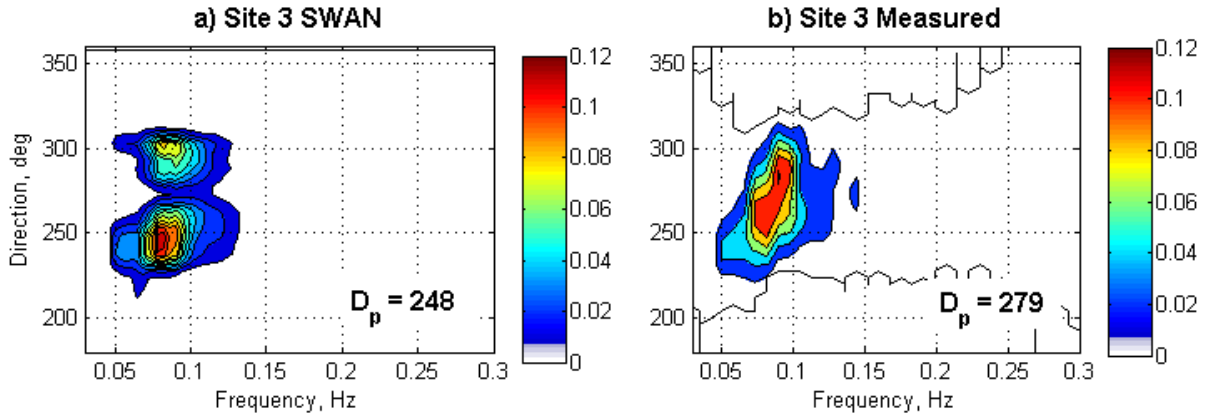

Figure 7. 2-D spectrum in m^2/Hz/deg a) modeled at site 3, b) measured at site 3 for test case 5.

3.2 Observed Beach Morphology Changes

Shoreline change rates were calculated for the fall and spring for each identified profile by comparing historic LIDAR data from 1997-1998 to recent topographic survey data (Barnard et al., 2007). Figure 8 shows that seasonal shoreline change rates along Ocean Beach switch from patterns of accretion to erosion at profile 80 (Barnard et al., 2007), which is located in reach 4, just north of the 4177 km northing location (Figure 5a). The average shoreline change rate from April 1997 to 2006 for profiles 1 to 79 is 1.1 m/yr and for profiles 80 to138 is -0.9 m/yr. Average profile statistics determined for each topographic profile also indicate a change at that location, and they are superimposed on local bathymetry in Figure 9. The swash beach width and sediment storage show a similar pattern with decreasing values southward, north of reach 4 (Figure 9a,b). They both show an increase at reach 4, more drastically for sediment storage. The beach slope also shows a sharp increase at reach 4, and slopes north and south of this location are relatively constant (Figure 9c). These changes in beach morphology occur just south of the location where the ebb tidal delta connects with the shore, creating a shallower section in approximately ten meters of water. The erosion hotspot is located further south, centered at a northing of 4176 km and at the location where there is a sharp decrease in beach width and subsequently sediment storage.

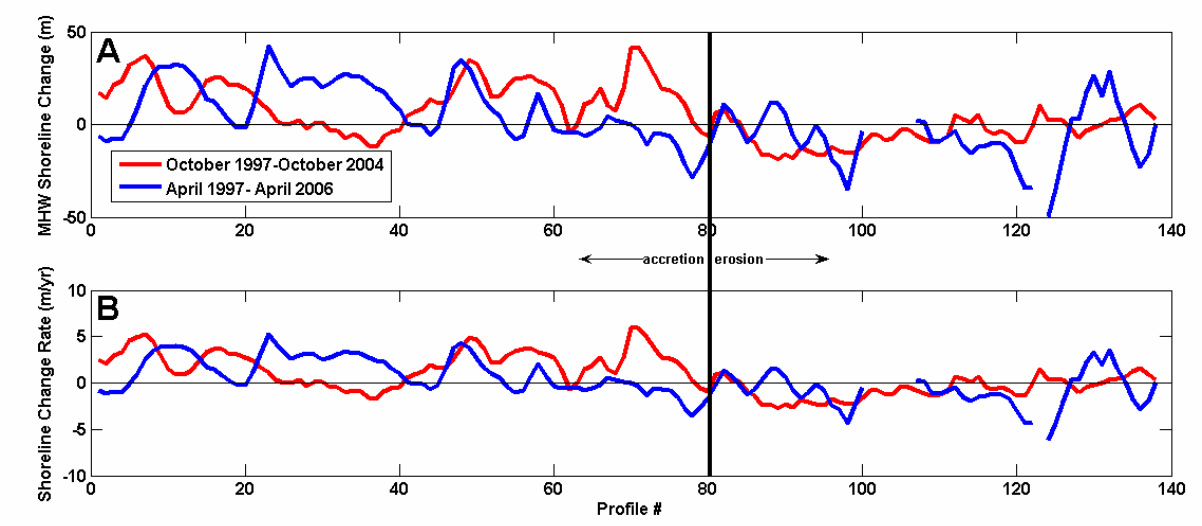

Figure 8. Shoreline change since LIDAR data was collected in 1997-98. a) Change in the MHW location and b) change in the shoreline change rate. The red line represents the rate as determined from the fall beach (October 1997 - October 2004). The blue line represents the rate as determined from the spring beach (April 1997 - April 2006). Figure from Barnard et al., 2007.

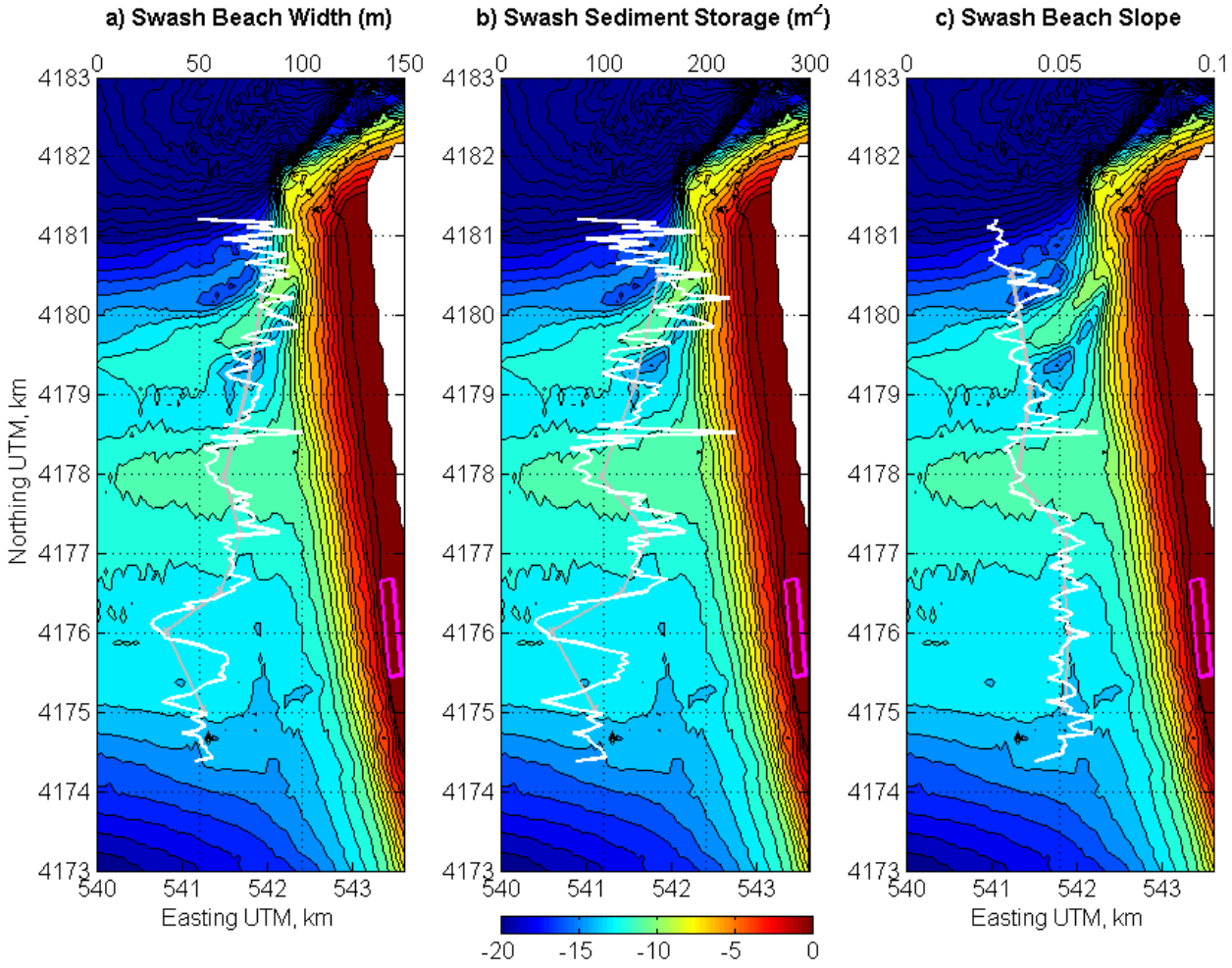

Figure 9. Average values of a) swash beach width, m b) swash sediment storage m^2 and c) swash beach slope averaged over the profile for each individual profile (white line) and also by reach (gray line) plotted on local bathymetry. Magenta box shows location of erosion hotspot.

3.3 Impact of incident wave angle at Ocean Beach

Ocean Beach is located in an environment exposed to a wide range of incident wave angles and a significant amount of very low frequency energy, which has a strong impact on the amount of energy that is transferred to the nearshore region. Data from 1996 through the present recorded at the CDIP buoy #029 show that offshore incident wave directions can vary as much as 180˚ over a typical year. Angle histograms of wave height by month determined from this data show that the majority of incidence angles are between 300˚ and 330˚, but in winter months there are a much higher percentage of waves directed onshore between 270˚ and 300˚, and in the summer, south swell ranges from 180˚ to 210˚ (Figure 10). Long period swell events are common and the recorded peak wave periods are greater than or equal to 15 seconds for 15% of the total record of data.

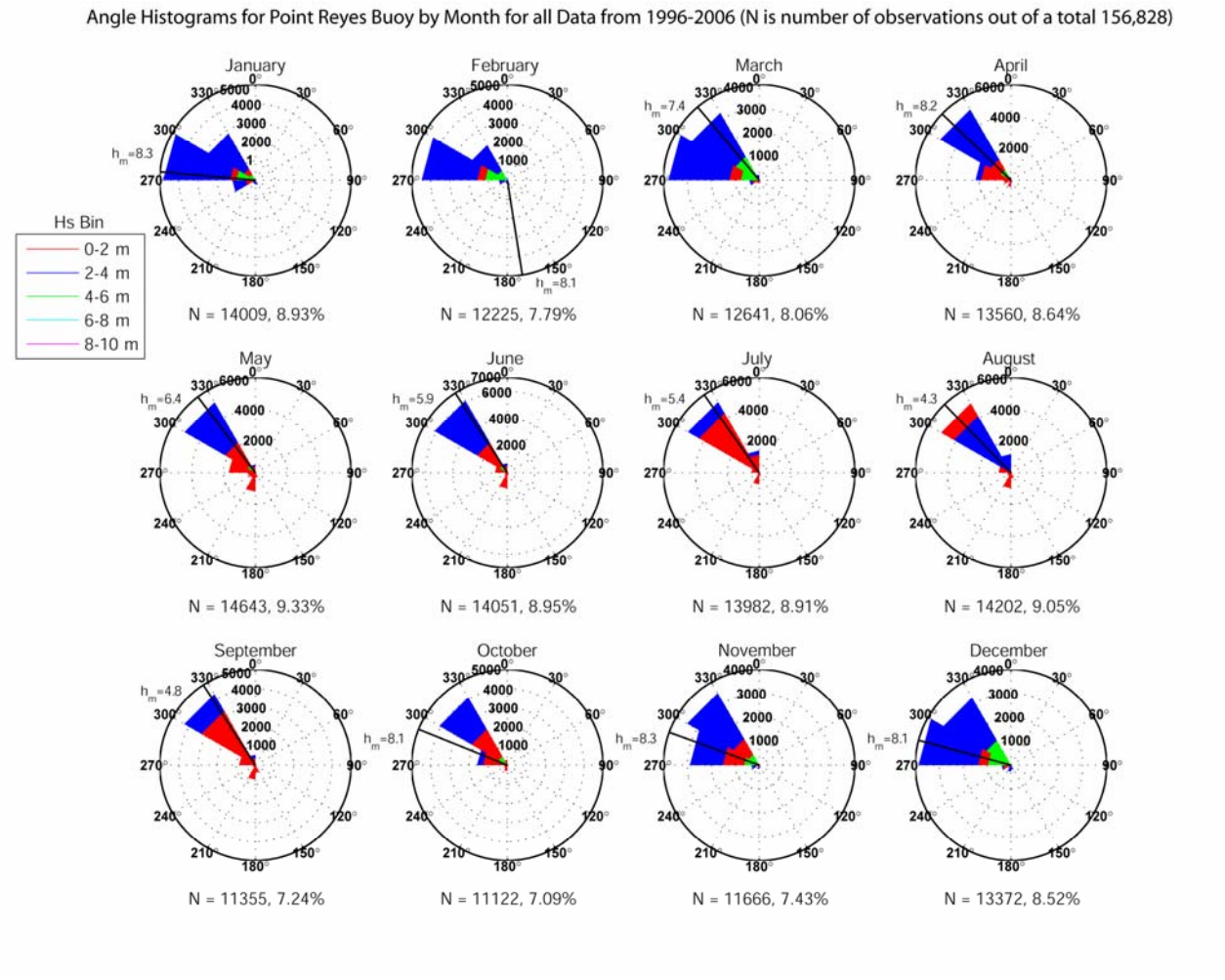

Figure 10. Direction histograms for Point Reyes CDIP buoy #029 by month for all available wave data measured from 1996 through 2006 (N is number of observations out of a total 156,828, the percentage is for the total data that occurred in that month, and h_m is the maximum wave height for the month which came from a direction marked by the solid black line; Scripps, 2006).

In order to better understand the effects of offshore wave forcing on the nearshore wave climate, bins of significant wave height, peak wave period, and peak wave direction were generated based on the available record of wave data measured at CDIP buoy #029. The bins are equally spaced with 0.5 m resolution for significant wave height, 10 degree resolution for peak wave direction, and 2 s resolution for peak wave period. Figure 11 shows probability density functions of the CDIP buoy data along with the specified bin boundaries in wave height period and direction. Bins with physically unrealistic combinations of significant wave height, peak wave period, and peak wave direction were removed from the analysis. The calibrated SWAN model was run with each possible binned combination, resulting in 4577 model runs. The results were compiled in a look up table using a similar technique to that employed by Ruggiero et al. (2006) to generate local wave input for shoreline change modeling. The look up table gives bulk wave parameter outputs at each of the topographic profiles along the 10 m contour for all binned offshore wave conditions. For this approach, constant parameterized forcing using a Jonswap spectrum with a

default peak enhancement factor and a power of 10 for spreading was applied on the north, west and south boundaries and currents were not included in the model.

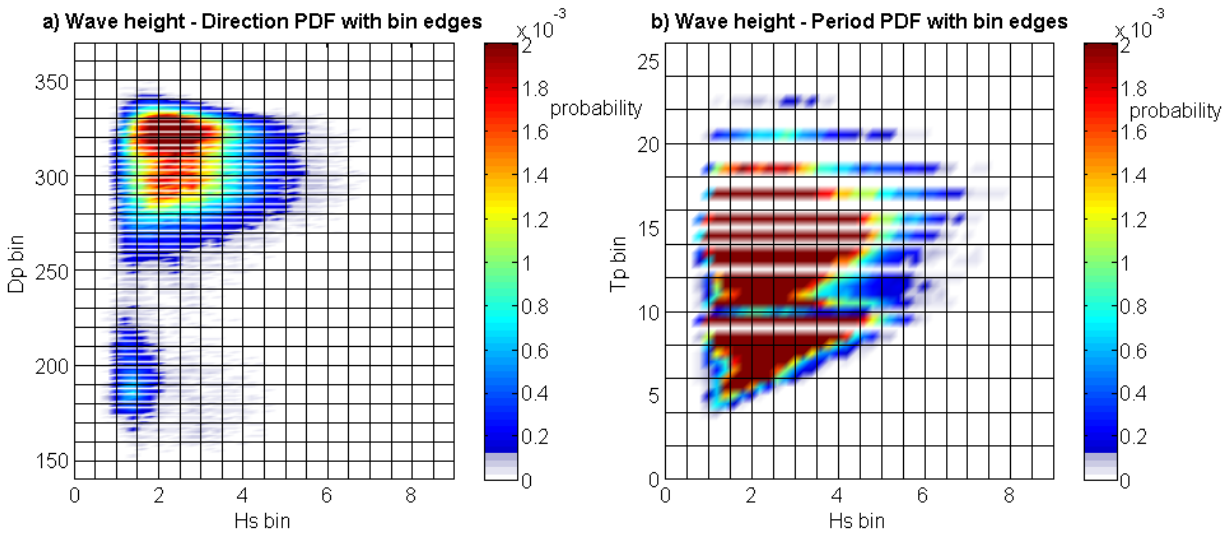

Figure 11. Probability density function of a) significant wave height and peak wave direction with bin edges and b) significant wave height and peak wave period with bin edges generated from available data measured at the CDIP buoy #029 from 1996 to present (Scripps, 2006).

Figure 12 includes plots of significant wave height output along the 10 m depth contour averaged over a range of peak directions. The significant wave height values represent an average of look up table output for all offshore binned wave heights and periods that fall into the specified range of direction bins. For example, the magenta line in Figure 12 represents an average of 10 m contour output for all model runs with peak wave directions between 240˚ and 270˚ applied at the offshore boundary. This is an average value for all wave heights (ranging from 0.5 to 9m) and all wave periods (ranging from 2 to 26 s) applied at the offshore boundary. The goal of this exercise is to identify alongshore gradients in energy that result from different offshore forcing peak wave directions.

There are very strong gradients in average significant wave height alongshore for all different groupings of direction bins. Average wave height contours for all groupings of direction bins greater than 270˚ have similar alongshore shape. For these northerly angles of incidence (270˚ to 10˚), wave height values drop off at the northern and southern portions of the beach (reaches 1 and 7), and the energy is focused in the central region (reaches 2-6), with a maximum at the boundary of reaches 2 and 3 (Figure 12). As expected, we see that the more onshore directed the angle is, the greater the wave height output. Average wave height contours for all groupings of direction bins less than 270˚ can also be grouped with similar alongshore shape. For southerly angles (180˚ to 270˚), reach 1 receives the most energy, with wave heights up to a half meter higher than anywhere else along the beach. There is a very large drop in wave height at a northing of 4180, which is located at a shallow section off of the beach (Figure 9) and at the southern end of reach 1 (Figure 12). Perhaps the bathymetry provides sheltering effects at this location. Although average significant wave height contour shapes can be grouped based on offshore incident angle relative to 270˚, the magnitudes in the central portion of the beach

(reaches 3-5) are greatest for onshore directions (210˚-300˚), and nearshore modeled wave heights are smaller as offshore incidence angles move outside of this range due to increased refraction.

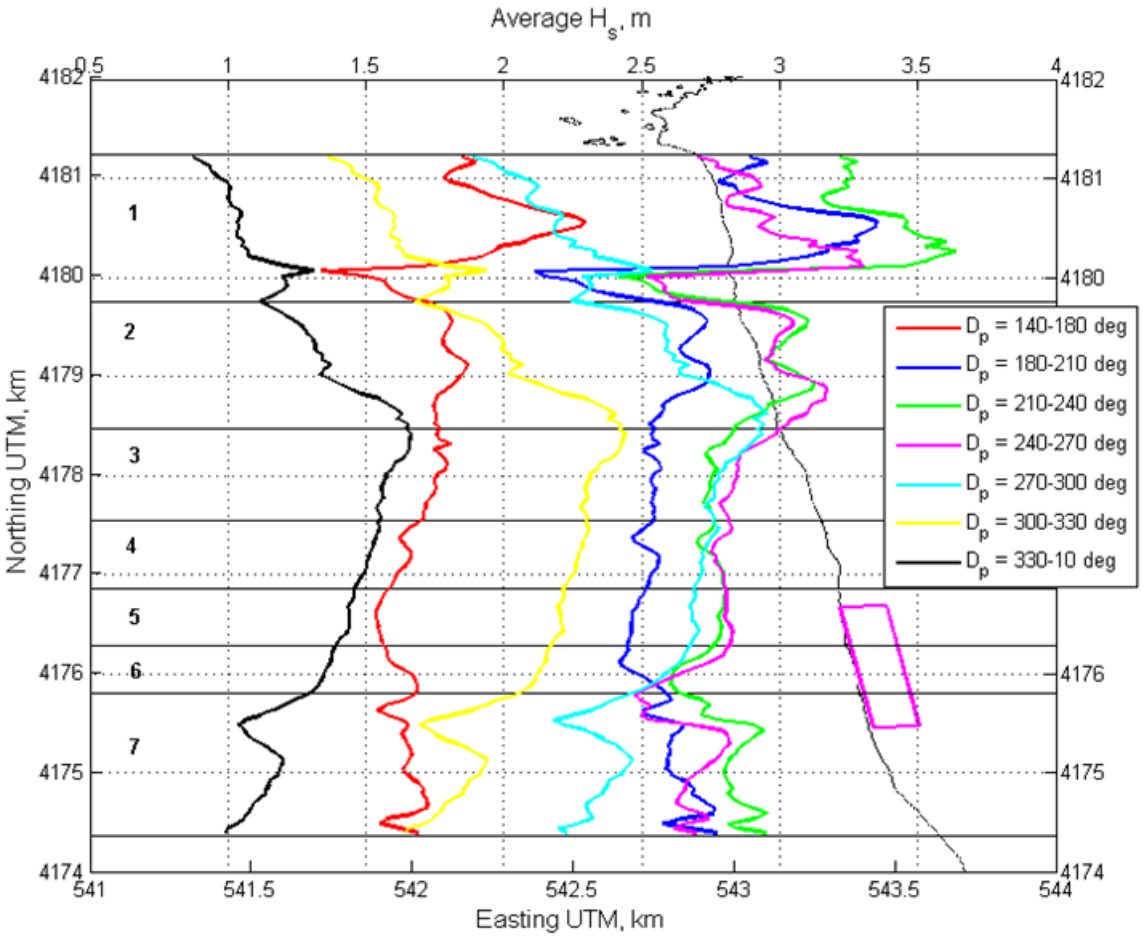

Figure 12. Alongshore varying mean (colored lines) of significant wave height at the 10 m depth contour for all bins within the specified peak direction range plotted versus the Ocean Beach shoreline and reach designations for comparison. Magenta box shows location of erosion hotspot.

The offshore wave period applied at the boundary also influences modeled wave heights at Ocean Beach because longer period waves will have different refraction patterns. This relationship is illustrated in Figure 13, which includes averages of modeled contour output for different wave period and wave direction groupings. This plot is similar to Figure 12, however now the averaged output over different direction bins has been further separated into different period ranges. For example, the blue line in Figure 13a represents an average of 10 m contour output for all model runs with peak wave directions between 210˚ and 240˚ and peak wave periods between 5 and 10 s applied at the offshore boundary. In general, the differences in output wave height for different ranges of wave period are relatively constant alongshore (Figure 13). This is not true for the 300˚ to 330˚ wave direction bin, where the difference in wave height

output for different wave periods varies alongshore. At the southern end of the beach in reach 7, waves with periods of 10 seconds or greater give the same nearshore wave height irrespective of the wave period (Figure 13d). The rate of increase in nearshore modeled wave height caused by an increase in offshore wave period is slower for periods of 10 s or greater, evidenced by the more closely spaced contours for longer periods (Figure 13).

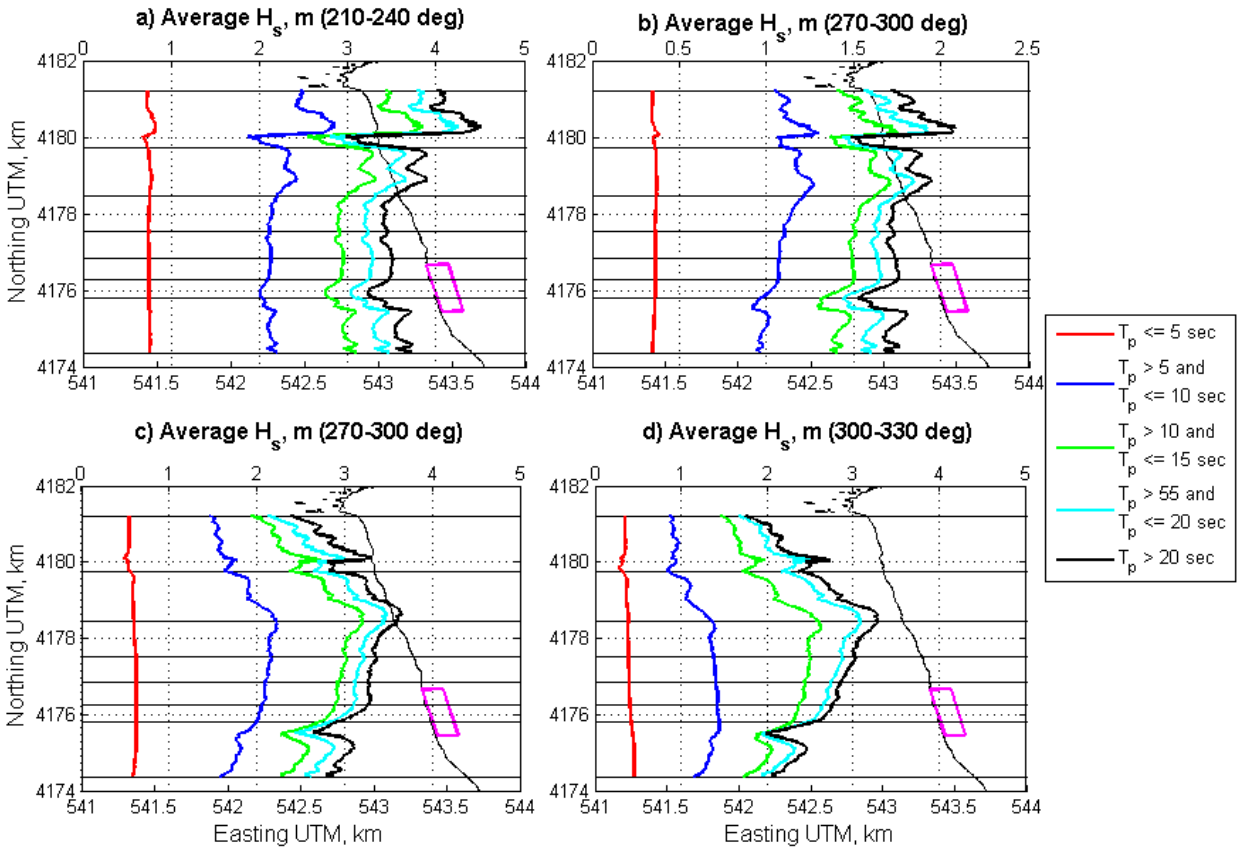

Figure 13. Alongshore varying mean (bold line) and standard deviation (dashed lines) of significant wave height at the 10 m depth contour for all bins within the specified peak period range for Dp bins from a) 210˚-240˚ b) 240˚-270˚ c) 270˚-300˚ and d) 300˚-330˚. Reach designations are plotted as black lines and the magenta box shows the location of the erosion hotspot.

4.0 Conclusions

Many recent data collection and modeling efforts have been focused at Ocean Beach in San Francisco, CA, to help understand and potentially mitigate the effects of an erosion hotspot at the southern end of the beach. The availability of detailed measurements of beach morphology over seasonal timescales makes it an ideal location to examine relationships between environmental forcing and beach response. In the southern end of the beach (south of profile 80) the upper swash limit cannot be defined, since the swash zone is cut off by cliff backing (Figure 5). This section has a much steeper swash beach slope, and although there is local recovery of beach width and sediment storage, these values drop off south of reach 5 (Figure 9). Shoreline change

rates calculated between 1997/98 and recent years show a change from accretion to erosion at profile 80 as well (Figure 8). Profile 80 is located just south of where the ebb tidal delta connects with the shore (Figure 9), resulting in a shallower section along the beach in approximately 10 m water depth. Changes in all beach parameters at the same location suggests that the bathymetry exerts a first order control over the location of the erosion hotspot, which is in the southern portion of the beach less than a kilometer south of profile 80. Average values of wave height output along the 10 m contour show focusing of increased energy in the northern portion of the beach (reaches 1 and 2) for angles of incidence less than 270˚ and in the central portion of the beach (from the southern half of reach 2 through the northern half of reach 6) for all angles of incidence. The erosion hotspot is located at the south end of this central focusing area, with only the northern tip within the focus area. This is the same location where waves with angles of incidence greater than 270˚ start to show a drop off in energy. The erosion hotspot is not located where wave energy is focused, but south of the focus section where there are strong gradients in wave energy alongshore.

Separating the wave model from other components of nearshore circulation enables an analysis of the impacts of different offshore wave conditions on the beach and provides a mechanism for identifying spatial variations that result from different combinations of offshore forcing. This approach compares specific common offshore wave scenarios in attempt to look at the full wave spectral output in detail and identify strengths and weaknesses of individual model processes. The wave model generally underestimates wave heights, but this is often because it overly dissipates the high frequency energy. Comparisons of measured and modeled frequency spectra show that it successfully captures changes in frequency and direction as waves refract over the ebb tidal delta, however bulk wave parameters are not effective at describing the wave climate since energy at multiple frequencies and directions is often present. The offshore wave direction and period have a very pronounced effect on output along Ocean Beach. Southerly angles show different spatial variation and exert strong pressure on the entire beach, whereas northerly angles focus energy on central reaches. Reaches 1, 2 and 7 are protected in a sense, since the majority of offshore incident wave angles are from the north.

One application of comparisons of waves from different directions is the effect of the 1997/1998 El Niño, when Pacific Northwest beaches experienced incident wave angles with a more southwest approach than typical (Kaminsky et al., 1998; Komar et al., 2000). The northern part of Ocean Beach experienced increased erosion during this winter (Barnard et al.,2007). Figure 12 suggests that increased southerly incident angles also impact the central portion of the beach because the amount of energy that reaches this region for southern incident angles is similar in magnitude to an onshore approach. Furthermore, longer offshore wave periods lead to increased nearshore wave heights. Allan and Komar (2006) show that there have been decadal increases in peak spectral wave periods along the entire West Coast, and although these are small, an increase in wave period may exert increased pressure on the entire beach.

The lookup table approach is a useful tool to help identify changes in nearshore wave patterns for changing offshore wave forcing. Future work aims to incorporate this wave model into a full 2d circulation model to look at varied sediment transport patterns along the beach. In addition, the nearshore wave information can be used as input for probabilistic shoreline change modeling for coastal hazard assessment (Ruggiero et al., 2006).

5.0 Acknowledgements

This research was supported by the United States Army Corps of Engineers, San Francisco District, the USGS Mendenhall Post-Doctoral Fellowship Program, and the USGS Coastal Evolution: Process-based Multi-scale Modeling Project. Thanks to Kathy Presto and Jon Warrick for their helpful review comments.

6.0 References

Allan, J.C. and Komar, P.D., 2006. Climate controls on US West Coast erosion processes. Journal of Coastal Research, 22(3): 511-529.

Aubrey, D.G., 1979. Seasonal patterns of onshore-offshore sediment movement. Journal of Geophysical Research-Oceans and Atmospheres, 84(NC10): 6347-6354.

Aubrey, D.G. and Ross, R.M., 1985. The quantitative description of beach cycles. Marine Geology, 69(1-2): 155-170.

Barnard, P.L., Eshleman, J.L., Erikson, L.H., and Hanes, D.M., 2007. Coastal processes study at Ocean Beach, San Francisco, CA: Summary of data collection 2004-2006. U.S. Geological Survey Open-File Report 2007-1217, 165 pp., http://pubs.usgs.gov/of/2007/1217/.

Birkemeier, W.A. and Mason, C., 1984. The Crab - A Unique Nearshore Surveying Vehicle. Journal Of Surveying Engineering-ASCE, 110(1): 1-7.

Dail, H.J., Merrifield, M.A. and Bevis, M., 2000. Steep beach morphology changes due to energetic wave forcing. Marine Geology, 162(2-4): 443-458.

Delft3D, 2006: Rotterdam, The Netherlands, WL Delft Hydraulics.

Delft University of Technology, 2007. SWAN Cycle III Version 40.51A User Manual, Delft, The Netherlands, 111 p, http://www.fluidmechanics.tudelft.nl/swan/index.htm.

Guillen, J., Stive, M.J.F. and Capobianco, M., 1999. Shoreline evolution of the Holland coast on a decadal scale. Earth Surface Processes And Landforms, 24(6): 517-536.

Jimenez, J.A., SanchezArcilla, A., Bou, J. and Ortiz, M.A., 1997. Analysing short-term shoreline changes along the Ebro delta (Spain) using aerial photographs. Journal of Coastal Research, 13(4): 1256-1266.

Kaminsky, G.M., Ruggiero, P., and Gelfenbaum, G., 1998. Monitoring coastal change in southwest Washington and northwest Oregon during the 1997/98 El Niño. Shore and Beach, 66(3), 42-51.

Katoh, K., 1997. Hazaki Oceanographical Research Station (HORS). Marine Technology Society Journal, 31(4): 49-56.

Komar, P.D., Allan, J.C., Dias-Mendez, G., Marra, J.J. and Ruggiero, P., 2000. El Niño and La Niña-erosion processes and impacts. Proceedings of the 27th International Conference on Coastal Engineering, ASCE, pp. 2414-2427.

Lacey, E.M. and Peck, J.A., 1998. Long-term beach profile variations along the south shore of Rhode Island, USA. Journal Of Coastal Research, 14(4): 1255-1264.

Larson, M. and Kraus, N.C., 1994. Temporal And Spatial Scales Of Beach Profile Change, Duck, North-Carolina. Marine Geology, 117(1-4): 75-94.

National Marine Sanctuary Program, 2003. Multibeam and echosounder data. http://squid.wr.usgs.gov/internal/MCSDevelop/cencalGIS/catalog.html

Norcross, Z.M., Fletcher, C.H. and Merrifield, M., 2002. Annual and interannual changes on a reef-fringed pocket beach: Kailua Bay, Hawaii. Marine Geology, 190(3-4): 553-580.

Ruggiero, P., Kaminsky, G.M., Gelfenbaum, G. and Voigt, B., 2005. Seasonal to interannual morphodynamics along a high-energy littoral cell. Journal of Coastal Research, 21(3): 553-578.

Ruggiero, P., List, J., Hanes, D., Eshleman, J., 2006. Probabilistic shoreline change modeling, San Diego, CA, Proceedings of the 30th International Conference on Coastal Engineering, ASCE.

SCRIPPS Institution of Oceanography, 2006. The Coastal Data Information Program. Integrative Oceanography Division, Scripps Institution of Oceanography, San Diego.

Shepard, F.P., 1950. Beach cycles in southern California. Beach Erosion Board, United States Army Corps of Engineers Technical Memo 20: 26 pp.

Sonu, C.H., and Van Beek, J.L., 1971. Systematic Beach Changes on the Outer Banks, North Carolina. Journal of Geology, 79: 416-425.

Winant, C.D., Inman, D.L. and Nordstrom, C.E., 1975. Description Of Seasonal Beach Changes Using Empirical Eigenfunctions. Journal Of Geophysical Research, 80(15): 1979-1986.

Wright, L.D., Short, A.D., and Green, M.O., 1985. Short-term changes in the morphodynamic states of beaches and surf zones: An empirical predictive model. Marine Geology, 62: 339-364.

Yates, M., Guza, R.T., Seymour, R.J., O'Reilly, W.C. and Thomas, J.O., in press. Seasonal changes in sand level and wave energy in Southern California. In: A.S.o.C. Engineers (Editor), ICCE 2006 Conference Proceedings, San Diego, CA, pp. 14.